THE JOURNAL OF PHYSICAL CHEMISTRY A

Article

pubs.acs.org/JPCA

Matrix Isolation Spectroscopic and Theoretical Study of Carbon Dioxide Activation by Titanium Oxide Molecules

Jia Zhuang, Zhen Hua Li,* Kangnian Fan, and Mingfei Zhou*

Department of Chemistry, Shanghai Key Laboratory of Molecular Catalysts and Innovative Materials, Fudan University, Shanghai 200433, China

Supporting Information

ABSTRACT: The reactions of titanium monoxide and dioxide molecules with carbon dioxide were investigated by matrix isolation infrared spectroscopy. It was found that the titanium monoxide molecule is able to activate carbon dioxide to form the titanium dioxide−carbon monoxide complex upon visible light excitation via a weakly bound TiO(η^1-OCO) intermediate in solid neon. In contrast, the titanium dioxide molecule reacted with carbon dioxide to form the titanium monoxide−carbonate complex spontaneously on annealing. Theoretical calculations predicted that both activation processes are thermodynamically exothermic and kinetically facile.

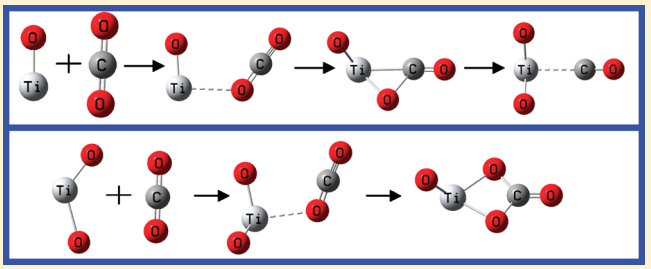

INTRODUCTION

The interactions of transition metal atoms, cations, and anions as well as simple metal oxide molecules with CO_2 serve as the simplest model in understanding the intrinsic mechanism of catalytic CO_2 activation processes. The reactions of atomic transition metal cations and neutrals with carbon dioxide have been intensively studied both experimentally and theoretically. Gas phase kinetic studies on the reactions between atomic transition metal cations and CO_2 showed that early transition metal cations are able to activate CO_2 in forming metal monoxide cation and CO, whereas the other transition metal cations form adducts with CO_2.[1−6] Matrix isolation spectroscopic as well as gas phase kinetic investigations have been performed on the reactions of neutral transition metal atoms with CO_2, which indicated that the ground state early transition metal atoms were able to activate the C═O bond of CO_2 in forming the inserted OMCO molecules, whereas the late transition metal atoms interacted with CO_2 to give either the η^1-C or η^1-O coordination complexes.[7−15] Besides the experimental studies, quantum chemical calculations have also been performed to understand the reaction mechanisms as well as the structural and bonding properties of the resulting complexes.[16−20] In contrast, the reactions between transition metal oxides and carbon dioxide have received much less attention. The reactivity of simple transition metal oxide cations such as monoxide cations with CO_2 has been studied in the gas phase. The MO_2^+ dioxide formation by O atom transfer occurred with NbO^+, HfO^+, TaO^+, and WO^+.[5,6] CO_2 reduction by group 6 transition metal suboxide cluster anions was reported.[21] CO_2 coordination and activation by niobium oxide molecules were studied in this laboratory, which showed that the niobium monoxide molecule is able to activate carbon dioxide to form NbO_2(η^1-CO) in solid neon; in contrast, the niobium dioxide molecule reacted with carbon dioxide to form complexes with three different coordination modes.[22] In this paper, we report a combined matrix isolation infrared spectroscopic and theoretical study of the reactions of titanium monoxide and dioxide molecules with carbon dioxide. Titanium oxide based materials are currently intensively studied as catalysts for photoinduced activation of CO_2.[23] Although CO_2 adsorption and photoreduction on titanium oxide surfaces have been well studied both experimentally and theoretically,[24] there is no experimental report on reactions between CO_2 and molecular titanium oxides, which provides a prototype system in understanding the mechanism of carbon dioxide activation by titanium oxides.

EXPERIMENTAL AND COMPUTATIONAL METHODS

The titanium monoxide and dioxide molecules were prepared by pulsed laser evaporation of bulk titanium dioxide target. Recent investigations in our laboratory have shown that pulsed laser evaporation is an effective method in preparing transition metal monoxide or dioxide molecules for matrix isolation spectroscopic studies.[25−27] The experimental setup for pulsed laser evaporation and matrix isolation infrared spectroscopic investigation has been described in detail previously.[28] Briefly, the 1064 nm fundamental of a Nd:YAG laser (Continuum, Minilite II, 10 Hz repetition rate and 6 ns pulse width) was focused onto a rotating titanium dioxide target through a hole in a CsI window cooled normally to 4 K by means of a closed-cycle helium refrigerator. The laser-evaporated metal oxide

Received: January 31, 2012
Revised: March 15, 2012
Published: March 15, 2012

   dx.doi.org/10.1021/jp301025n | J. Phys. Chem. A 2012, 116, 3388−3395

species were codeposited with CO_2/Ne mixtures onto the CsI window. In general, matrix samples were deposited for 30 min at a rate of approximately 4 mmol/h. The bulk TiO_2 target was prepared from sintered metal oxide powder. The CO_2/Ne mixtures were prepared in a stainless steel vacuum line using standard manometric techniques. Isotopically labeled $^{13}CO_2$ (Spectra Gases Inc., 99%), $C^{18}O_2$ (Cambridge Isotopic Laboratories, 95%), and $C^{16}O_2$ + $C^{16}O^{18}O$ + $C^{18}O_2$ (Cambridge Isotopic Laboratories, 61% ^{18}O) were used without further purification. The infrared absorption spectra of the resulting samples were recorded on a Bruker IFS 80 V spectrometer at 0.5 cm^{-1} resolution between 4000 and 450 cm^{-1} using a liquid nitrogen cooled HgCdTe (MCT) detector. Samples were annealed to different temperatures and cooled back to 4 K for spectral acquisition, and selected samples were subjected to broad band irradiation using a high-pressure mercury arc lamp with glass filters.

Quantum chemical calculations were performed to determine the molecular structures and to support the assignment of vibrational frequencies of the observed reaction products. The calculations were performed with the B3LYP density functional theory (DFT) method, where Becke's three-parameter hybrid functional and the Lee−Yang−Parr correlation functional were used.[29] The basis set used is 6-311+G(2df).[30] The B3LYP functional is the most popular density functional methods and can provide reliable predictions on the structures and vibrational frequencies of early transition metal-containing compounds.[31] Our test calculations indicated that for the system studied here it can give similar results as the more expensive double-hybrid method. The geometries of various reactants, intermediates, and products were fully optimized, and the harmonic vibrational frequencies were calculated with analytic second derivatives. The zero-point energies (ZPE) were derived. Transition state optimizations were done with the synchronous transit-guided quasi-Newton (STQN) method and were verified through intrinsic reaction coordinate (IRC) calculations.[32] All these calculations were performed by using the Gaussian 09 program.[33]

RESULTS AND DISCUSSION

Infrared Spectra. Pulsed laser evaporation of bulk TiO_2 target under controlled laser energy (2−5 mJ/pulse) followed by condensation with pure neon formed only the TiO (997.9 cm^{-1} for ^{48}TiO) and TiO_2 (ν_3, 936.7 cm^{-1}; ν_1, 962.9 cm^{-1} for $^{48}TiO_2$) molecules. No other oxide species were observed.[34,35] The spectra in selected regions from codeposition of laser-evaporated titanium oxides with a 0.1% CO_2/Ne sample are shown in Figures 1 and 2, respectively. Besides the strong CO_2 absorptions (antisymmetric CO_2 stretching, 2347.7 cm^{-1}; bending, 668.0 cm^{-1}), the TiO and TiO_2 absorptions dominated the spectrum after sample deposition at 4 K. New product absorptions were produced when the as-deposited sample was annealed, which can be classified into two groups (labeled as **A** and **B** in Figures 1 and 2). When the sample was subjected to visible light irradiation using the high pressure mercury lamp with a 500 nm long-wavelength pass filter (500 < λ < 580 nm), the group **A** absorptions were almost destroyed with the production of a new group of absorptions (labeled as **C** in Figures 1 and 2). The group **B** absorptions remain almost unchanged under visible light irradiation. Besides the absorptions in the spectral ranges shown in Figures 1 and 2, species **A** exhibits additional absorptions in the antisymmetric CO_2 stretching and bending vibrational frequency regions.

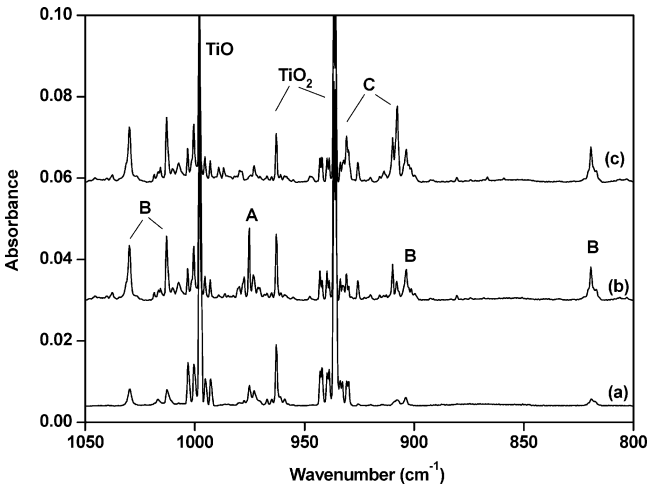

Figure 1. Infrared spectra in the 1050−800 cm^{-1} region from codeposition of laser-evaporated titanium oxides with 0.1% CO_2 in neon (a) 30 min of sample deposition at 4 K, (b) after 12 K annealing, and (c) after 15 min of visible light (500 < λ < 580 nm) irradiation. **A**, TiO(η^1-OCO); **B**, $OTiCO_3$; **C**, TiO_2(η^1-CO).

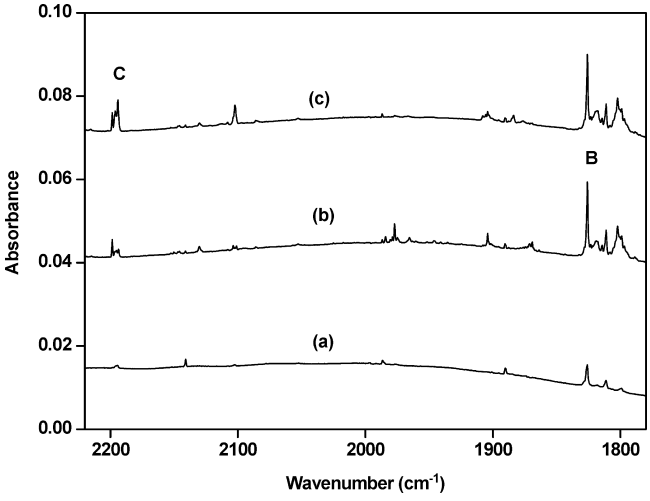

Figure 2. Infrared spectra in the 2220−1780 cm^{-1} region from codeposition of laser-evaporated titanium oxides with 0.1% CO_2 in neon (a) 30 min of sample deposition at 4 K, (b) after 12 K annealing, and (c) after 15 min of visible light (500 < λ < 580 nm) irradiation. **B**, $OTiCO_3$; **C** TiO_2(η^1-CO).

These absorptions are overlapped by the strong CO_2 absorptions but can be well resolved from the difference spectrum (spectrum taken after visible light irradiation minus spectrum taken after annealing) shown in Figure 3. Similar experiments with isotopic-labeled samples ($^{13}CO_2$, $^{12}CO_2$ + $^{13}CO_2$, $C^{18}O_2$ and $C^{16}O_2$ + $C^{16}O^{18}O$ + $C^{18}O_2$) were also done for product identification based on isotopic shifts and splitting. The spectra in selected regions with different isotopic samples are shown in Figures 4−6. The band positions and assignments of the observed product absorptions are summarized in Table 1.

TiO(η^1-OCO). The group **A** absorptions were produced on annealing. The relative intensities of the 980.5, 977.6, 975.3, 973.0, and 970.5 cm^{-1} absorptions match the natural abundance titanium isotopic intensity distributions and clearly indicate the involvement of one titanium atom. The band positions and titanium isotopic shifts imply that these

dx.doi.org/10.1021/jp301025n | J. Phys. Chem. A 2012, 116, 3388−3395

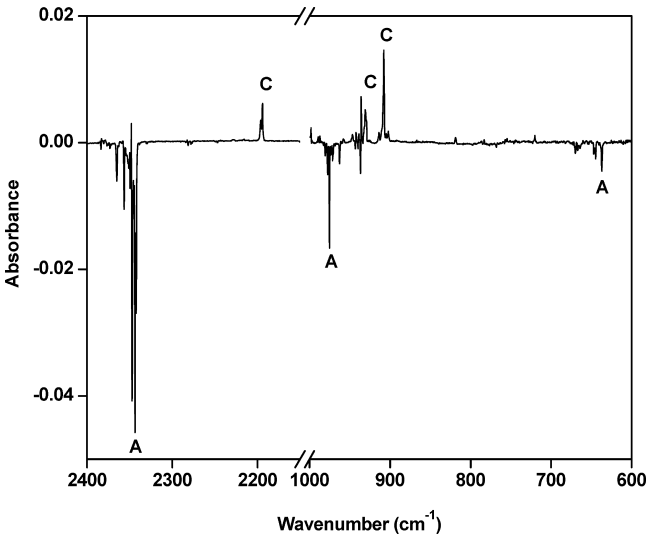

Figure 3. Difference IR spectrum in the 2400−2150 and 1000−600 cm^{-1} regions from codeposition of laser-evaporated titanium oxides with 0.05% CO_2 in neon. Spectrum was taken after 15 min of visible light (500 < λ < 580 nm) irradiation minus spectrum taken after 12 K annealing. **A**, TiO(η^1-OCO); **C**, TiO_2(η^1-CO).

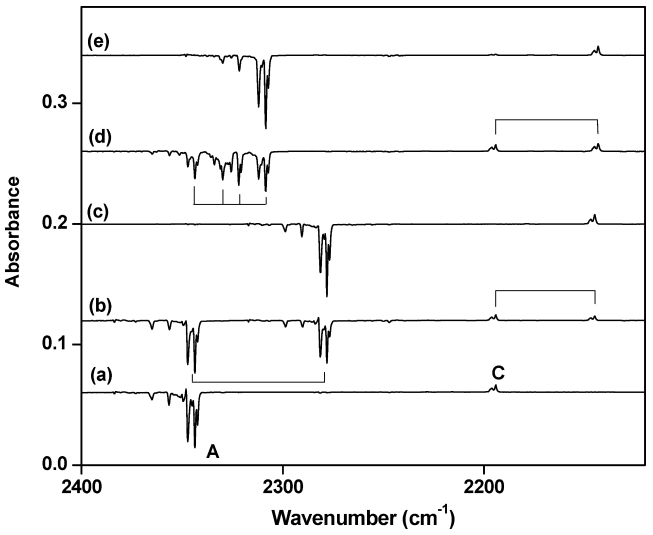

Figure 4. Difference IR spectrum in the 2400−2120 cm^{-1} region from codeposition of laser-evaporated titanium oxides with carbon dioxide in excess neon. Spectrum was taken after 15 min of visible light (500 < λ < 580 nm) irradiation minus spectrum taken after 12 K annealing: (a) 0.05% CO_2/Ne; (b) 0.05% $^{12}CO_2$ + 0.05% $^{13}CO_2$/Ne; (c) 0.05% $^{13}CO_2$/Ne; (d) 0.1% ($C^{16}O_2$ + $C^{16}O^{18}O$ + $C^{18}O_2$)/Ne (61%^{18}O); (e) 0.05%$C^{18}O_2$/Ne. **A**, TiO(η^1-OCO); **C**, TiO_2(η^1-CO).

absorptions are due to terminal Ti═O stretching vibrations. The band position for the most intense absorption (975.3 cm^{-1} for ^{48}Ti) is about 22.6 cm^{-1} red-shifted from that of diatomic TiO in solid neon. The 2343.7 cm^{-1} absorption shifted to 2278.0 cm^{-1} with $^{13}CO_2$ and to 2308.4 cm^{-1} with $C^{18}O_2$. The band position and isotopic frequency shifts indicate that this absorption is due to an antisymmetric CO_2 stretching vibration. The spectra from the experiments with the $^{12}CO_2$ + $^{13}CO_2$ and $C^{16}O_2$ + $C^{16}O^{18}O$ + $C^{18}O_2$ mixtures (Figure 4) clearly indicate that one CO_2 fragment with two inequivalent O atoms is involved in this mode. The 1354.7 cm^{-1} absorption is the symmetric stretching mode and the 644.7 and 637.0 cm^{-1}

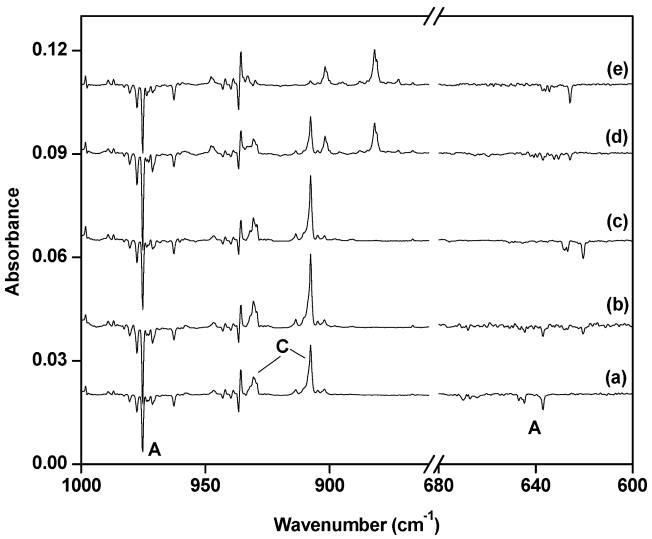

Figure 5. Difference IR spectrum in the 1000−860 and 680−600 cm^{-1} regions from codeposition of laser-evaporated titanium oxides with carbon dioxide in excess neon. Spectrum was taken after 15 min of visible light (500 < λ < 580 nm) irradiation minus spectrum taken after 12 K annealing: (a) 0.05% CO_2/Ne; (b) 0.05% $^{12}CO_2$ + 0.05% $^{13}CO_2$/Ne; (c) 0.05% $^{13}CO_2$/Ne; (d) 0.1% ($C^{16}O_2$ + $C^{16}O^{18}O$ + $C^{18}O_2$)/Ne (61%^{18}O); (e) 0.05%$C^{18}O_2$/Ne. **A**, TiO(η^1-OCO); **C**, TiO_2(η^1-CO).

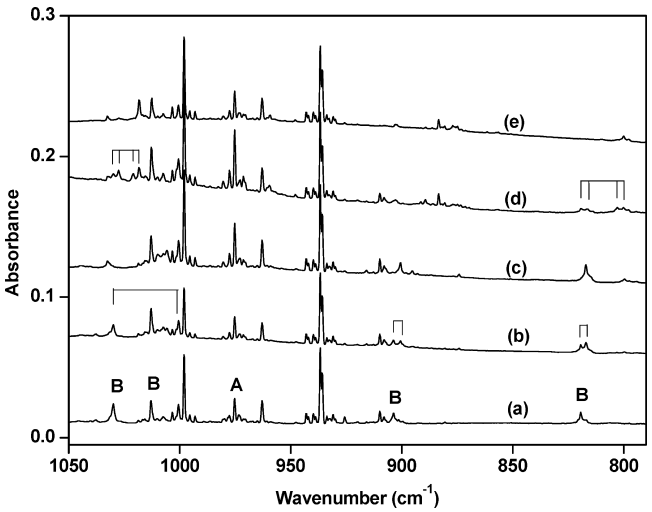

Figure 6. Infrared spectra in the 1050−790 cm^{-1} region from codeposition of laser-evaporated titanium oxides with carbon dioxide in excess neon. Spectra were taken after 12 K annealing: (a) 0.05% CO_2/Ne; (b) 0.05% $^{12}CO_2$ + 0.05% $^{13}CO_2$/Ne; (c) 0.05% $^{13}CO_2$/Ne; (d) 0.1% ($C^{16}O_2$ + $C^{16}O^{18}O$ + $C^{18}O_2$)/Ne (61%^{18}O); (e) 0.05% $C^{18}O_2$/Ne; **A**, TiO(η^1-OCO); **B**, $OTiCO_3$.

absorptions are the bending vibrations of the CO_2 fragment. These spectral features lead us to assign the group **A** absorptions to different vibrational modes of a TiO(η^1-OCO) complex with CO_2 coordinated to the Ti center in a η^1-O end-on fashion (Table 1). Previous studies indicate that CO_2 interacted with TiO_2 surface weakly forming linearly adsorbed species. The antisymmetric CO_2 stretching frequency for linear CO_2 on TiO_2 rutile (110) surface was observed at 2340 cm^{-1}, very close to that of the TiO(η^1-OCO) complex.[36]

To validate the experimental assignment, quantum chemical calculations using the density functional theory were

dx.doi.org/10.1021/jp301025n | J. Phys. Chem. A 2012, 116, 3388−3395

Table 1. Infrared Absorptions (cm^{-1}) from Codeposition of Titanium Oxides with Carbon Dioxide in Solid Neon

$^{12}C^{16}O_2$	$^{13}C^{16}O_2$	$^{12}C^{18}O_2$	$C^{16}O_2 + C^{16}O^{18}O + C^{18}O_2$	assignment
2347.2	2281.2	2312.0	2347.1, 2334.1, 2325.6, 2312.0	TiO(η^1-OCO) site
2343.7	2278.0	2308.4	2343.7, 2329.8, 2321.9, 2308.4	TiO(η^1-OCO) antisym CO_2 str
1354.7	1345.0			TiO(η^1-OCO) sym CO_2 str
980.5				^{46}TiO(η^1-OCO) Ti=O str
977.6				^{47}TiO(η^1-OCO) Ti=O str
975.3	975.2	975.2		^{48}TiO(η^1-OCO) Ti=O str
973.0				^{49}TiO(η^1-OCO) Ti=O str
970.5				^{50}TiO(η^1-OCO) Ti=O str
644.7	626.8	634.4		TiO(η^1-OCO) CO_2 bend.
637.0	620.4	625.8	637.0, 632.4, 630.5, 625.8	TiO(η^1-OCO) CO_2 bend.
2194.2	2145.0	2143.2	2194.2, 2143.2	TiO_2(η^1-CO) CO str
930.8	930.7	901.9	930.8, 901.9	TiO_2(η^1-CO) sym TiO_2 str
913.7				$^{46}TiO_2$(η^1-CO) antisym TiO_2 str
910.6				$^{47}TiO_2$(η^1-CO) antisym TiO_2 str
907.7	907.7	882.0	907.7, 882.0	$^{48}TiO_2$(η^1-CO) antisym TiO_2 str
904.8				$^{49}TiO_2$(η^1-CO) antisym TiO_2 str
902.2				$^{50}TiO_2$(η^1-CO) antisym TiO_2 str
1825.9	1768.3	1785.7		$OTiCO_3$ CO str
1029.9	1000.5	1018.2	1029.9, 1027.5, 1020.9, 1018.2	$OTiCO_3$ antisym CO str
1018.6				$O^{46}TiCO_3$ Ti=O str
1015.6				$O^{47}TiCO_3$ Ti=O str
1012.9	1012.9	1012.6		$O^{48}TiCO_3$ Ti=O str
1010.2				$O^{49}TiCO_3$ Ti=O str
1007.4				$O^{50}TiCO_3$ Ti=O str
903.7	900.5	877.0		$OTiCO_3$ sym CO str
819.5	817.1	800.2		$OTiCO_3$ in-plane CO_2 bend.
784.3	762.2	775.5		$OTiCO_3$ out-of-plane CO_2 bend.
458.5	456.1	450.0		$OTiCO_3$ TiO_2 str

performed. The TiO(η^1-OCO) complex was predicted to have a ^{3}A″ ground state with planar C_s symmetry possessing a nearly linear CO_2 ligand with an OCO bond angle of 178.4° (Figure 7). The CO_2 ligand is end-on bonded to TiO via one O atom with a Ti−O distance of 2.336 Å. The complex can be viewed as being formed via the ground state of TiO ($^3\Delta$) and CO_2. Natural bond orbital (NBO) analysis[37] indicated that TiO(η^1-OCO) is a weak donor−acceptor complex with the oxygen of CO_2 donates its lone-pair electrons to the empty 3d orbital of Ti. The CO_2 fragment donates about 0.05e to TiO. To understand the bonding character in the complexes, a Wiberg bond order analysis was carried out. The results are presented in Table 2. It can be seen from Table 2 that the bond between Ti and the oxygen of CO_2 in TiO(η^1-OCO) is 0.11, indicating that a weak chemical bond is formed. In addition, the bond order of Ti=O in the complex is 1.91, slightly smaller than that of free TiO (1.94), implying that the Ti=O bond is weakened upon CO_2 coordination. The calculated vibrational frequencies of the complex are compared with the experimental values in Table 3, which provide strong support for the identification of the complex.

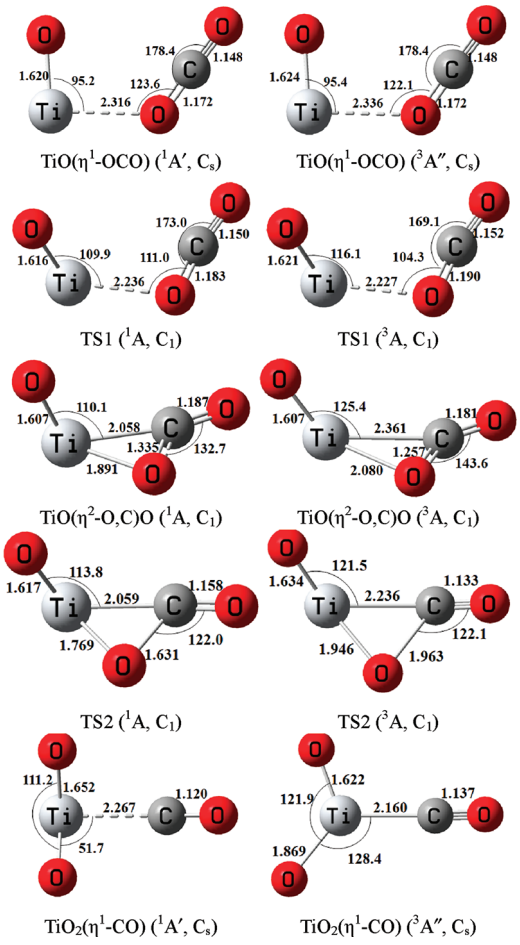

Figure 7. Optimized structures (bond lengths in Å and bond angles in degrees) of the intermediates and transition states involved in the TiO + CO_2 → TiO_2(η^1-CO) reaction.

Table 2. Wiberg Bond Order of the TiO and C−O Bonds Calculated at the B3LYP/6-311+G(2df) Level of Theory[a]

complex	Ti=O	Ti−O(CO)[b]	Ti−C	C−O[c]	
CO_2				1.88	
TiO	1.95				
TiO_2	1.91				
TiO(η^1-OCO)	1.93	0.11		1.98	1.73
$TiCO_3$		0.70		1.75	1.02
$OTiCO_3$	2.10	0.75		1.76	1.0
TiO_2(η^1-OCO)	1.93	0.17		2.01	1.71
TiO(η^2-O,C)O	2.09	0.78	0.75	1.82	1.09
TiO_2(η^1-CO)	1.93		0.03	2.33	

[a]The results listed are for the electronic ground state of the complexes. [b]Bond between Ti and the oxygen atom of the CO_2 ligand. [c]CO bond in the CO_2 or CO ligand.

TiO_2(η^1-CO). The group **C** absorptions were produced under visible light irradiation at the expense of the group **A** absorptions, which suggests that species **C** is due to a structural isomer of **A**. The 2194.2 cm^{-1} absorption shifted to 2145.0 cm^{-1} with $^{13}CO_2$ and to 2143.2 cm^{-1} with $C^{18}O_2$. The isotopic frequency ratios ($^{12}C/^{13}C$, 1.0229; $^{16}O/^{18}O$, 1.0238) indicate that this absorption is due to a C−O stretching vibration. The spectral features observed in the experiments with the $^{12}CO_2$ + $^{13}CO_2$ and $C^{16}O_2$ + $C^{16}O^{18}O$ + $C^{18}O_2$ mixtures (Figure 4) indicate that only one CO subunit is involved in this mode. The

dx.doi.org/10.1021/jp301025n | J. Phys. Chem. A 2012, 116, 3388−3395

Table 3. Observed Neon Matrix and Calculated (B3LYP/6-311+G(2df)) Vibrational Frequencies (cm^{-1}) for TiO(η^1-OCO) (A)[a]

	TiO(η^1-OCO)		TiO(η^1-O^{13}CO)		Ti^{16}O(η^1- ^{18}OC^{18}O)	
mode	obs	calcd	obs	calcd	obs	calcd
CO_2 asym str	2343.7	2408.5(887)	2278.0	2339.8	2308.4	2371.9
CO_2 sym str	1354.7	1358.5(5)	1345.0	1358.3		1280.8
Ti═O str	975.3	1015.2(222)	975.2	1015.1	975.2	1015.1
CO_2 bending	644.7	644.5(21)	626.8	627.0	634.4	633.6
CO_2 bending	637.0	641.3(22)	620.4	623.0	625.8	631.5

[a]The intensities are listed in parentheses in km/mol. Only the vibrations above 400 cm^{-1} are listed. The vibrational frequency of ground state TiO molecule was predicted to be 1043.5 cm^{-1}.

Table 4. Observed Neon Matrix and Calculated (B3LYP/6-311+G(2df)) Vibrational Frequencies (cm^{-1}) for TiO_2(η^1-CO) (C)[a]

	TiO_2(η^1-CO)		TiO_2(η^1-^{13}CO)		Ti^{16}O ^{18}O(η^1-C^{18}O)	
mode	obs	calcd	obs	calcd	obs	calcd
CO str	2194.2	2252.5(246)	2145.0	2201.5	2143.2	2199.2
TiO_2 sym str	930.8	1006.2(36)	930.7	1006.1	901.9	989.7
TiO_2 asym str	907.7	942.1(367)	907.7	942.1	882.0	917.2

[a]The intensities are listed in parentheses in km/mol. Only the vibrations above 400 cm^{-1} are listed. The vibrational frequencies of TiO_2 were predicted to be 1027.1 (ν_1), 979.5 (ν_3), and 342.1 cm^{-1} (ν_2) with 39:469:14 km/mol relative IR intensities.

930.8 and 907.7 cm^{-1} absorptions are appropriate for the symmetric and antisymmetric OTiO stretching vibrations, which are about 32.1 and 29.0 cm^{-1} red-shifted from the corresponding modes of TiO_2 in solid neon. The titanium isotopic splittings can clearly be resolved for the antisymmetric stretching mode. The symmetric and antisymmetric stretching modes shifted to 901.9 and 882.0 cm^{-1} when the $C^{18}O_2$ sample was used. In the experiment with the $C^{16}O_2$ + $C^{16}O^{18}O$ + $C^{18}O_2$ mixture (Figure 5), each mode splits into a doublet. The observed spectral features imply that one of the O atoms in the TiO_2 fragment originates from CO_2, indicating that species **C** is formed via the reaction of titanium monoxide with CO_2. Accordingly, the group **C** absorptions are assigned to different vibrational modes of TiO_2(η^1-CO), a structural isomer of the TiO(η^1-OCO) complex. In the previous experiments on the reaction of titanium atoms with carbon dioxide in solid argon, absorptions at 2190.4 and 895.2 cm^{-1} were tentatively assigned to the C−O stretching and antisymmetric TiO_2 stretching vibrations of the TiO_2(η^1-CO) complex.[11b]

The TiO_2(η^1-CO) complex was predicted to have a ^{1}A′ ground state with nonplanar C_s symmetry (Figure 7), in which the C atom is end-on bonded to the Ti center with a Ti−C distance of 2.267 Å. The ground state TiO_2(η^1-CO) complex can be viewed as the interaction between a $^1A_1$ TiO_2 fragment and a CO fragment. NBO analysis indicated that the CO ligand bares a positive charge of about 0.39e and the bond order between Ti and C is 0.03 (Table 2). In the NBO analysis the interaction between the "filled" Lewis-type NBO (donor) and "empty" non-Lewis-type NBO (acceptor) can be examined by the second-order perturbation theory analysis through estimating the stabilization energy $E(2)$ associated with delocalization ("2e-stabilization") from donor orbital to acceptor orbital.[37] The analysis indicated that there is essentially no CO to metal σ donation and metal to CO π back-donation. Therefore, the interaction between TiO_2 and CO is best described as electrostatic bonding that has been observed in "non-classical" transition metal carbonyl cation systems.[38−40] Such electrostatic bonding increases the CO stretching frequency. The CO stretching frequency of TiO_2(η^1-CO) is blue-shifted by 53.4 cm^{-1} from CO isolated in solid neon. The calculated frequencies at the optimized geometry of TiO_2(η^1-CO) provide good support for the identification of this complex. The C−O stretching and the symmetric and antisymmetric TiO_2 stretching vibrations were calculated at 2252.5, 1006.2, and 942.1 cm^{-1}, respectively. As listed in Table 4, the calculated isotopic frequency shifts also are in excellent agreement with the experimental observations.

$OTiCO_3$. The group **B** absorptions are assigned to different vibrational modes of $OTiCO_3$ (Table 1), a carbonate complex. The 1012.9 cm^{-1} absorption showed no shift with $^{13}CO_2$ and a very small shift (0.3 cm^{-1}) with $C^{18}O_2$, which is appropriate for a terminal Ti═O stretching vibration. The titanium isotopic splitting of this absorption is clear for only one Ti atom involvement. The 1825.9, 1029.9, 903.7, 819.5, and 784.3 cm^{-1} absorptions are characteristic for a carbonate complex.[41] The 1825.9 cm^{-1} absorption shifted to 1768.3 cm^{-1} with $^{13}CO_2$ and to 1785.7 cm^{-1} with $C^{18}O_2$. In the mixed $^{12}CO_2$ + $^{13}CO_2$ experiment, no intermediate absorption was observed. The isotopic shift and splitting indicate that the 1825.9 cm^{-1} absorption is due to a terminal C−O stretching vibration and only one CO subunit is involved. The 1029.9 and 903.7 cm^{-1} absorptions shifted to 1000.5 and 900.5 cm^{-1} with the $^{13}CO_2$ sample, and to 1012.6 and 877.0 cm^{-1} with the $C^{18}O_2$ sample. The isotopic data imply that these two absorptions are due to C−O stretching vibrations. In the experiment with the $C^{16}O_2$ + $C^{16}O^{18}O$ + $C^{18}O_2$ mixture (Figure 6), each mode splits into a quartet, suggesting the involvement of a CO_3 fragment. The 819.5 and 784.3 cm^{-1} absorptions are attributed to the in-plane and out-of-plane CO_2 bending vibrations.

The $OTiCO_3$ complex was predicted to have a ^{1}A′ ground state with nonplanar C_s symmetry (Figure 8). The CO_3 fragment bound to the Ti center in a η^2-O, O side-on fashion with two equivalent Ti−O bonds. Whereas the CO_3 subunit coordinates with the Ti center by forming two weak Ti−O bonds (bond length, 1.883 Å; Wiberg bond order, 0.75), the terminal Ti═O bond is strongly bonded with a bond length of 1.606 Å and a Wiberg bond order of 2.10. The $OTiCO_3$ complex can be regarded as an oxo titanium carbonate complex, $[(TiO)^{2+}(CO_3)^{2-}]$, that is, a TiO^{2+} dication coordinated by a CO_3^{2-} anion. Natural bond orbital (NBO) analysis indicated

dx.doi.org/10.1021/jp301025n | J. Phys. Chem. A 2012, 116, 3388−3395

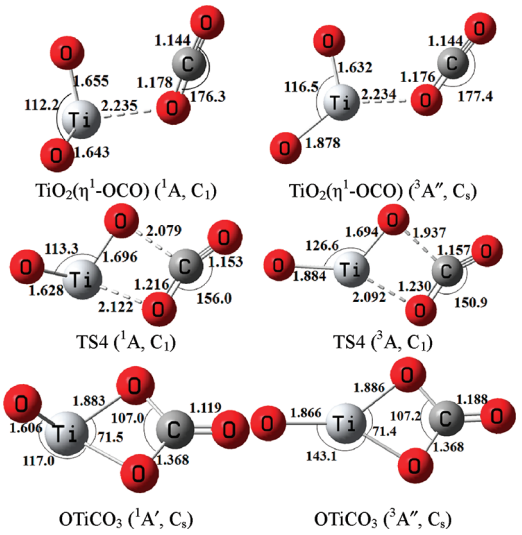

Figure 8. Optimized structures (bond lengths in Å and bond angles in degrees) of the intermediates and transition states involved in the $TiO_2 + CO_2 \rightarrow OTiCO_3$ reaction.

that the TiO subunit is positively charged with 1.01e, whereas the CO_3 fragment is negatively charged with −1.01e. The calculated vibrational frequencies of the $OTiCO_3$ complex are compared with the experimental values in Table 5, which provide strong support for the identification of the complex.

Reaction Mechanism. Pulsed laser evaporation of bulk TiO_2 target followed by condensation with CO_2 in excess neon at 4 K formed the TiO and TiO_2 molecules in the initial deposition. Annealing the deposited matrix sample allows the CO_2 molecules to diffuse and to react with the TiO and TiO_2 molecules. The isotopic substitution experimental results indicate that the TiO(η^1-OCO) complex was formed via the reaction between TiO and CO_2, reaction 1, whereas the $OTiCO_3$ complex was produced via the reaction of TiO_2 with CO_2, reaction 2. The production of TiO(η^1-OCO) and $OTiCO_3$ upon annealing suggests that both reactions require negligible activation energy.

$$TiO(^3\Delta) + CO_2(^1\Sigma_g^+) \rightarrow TiO(\eta^1\text{-}OCO)(^3A'') \quad \Delta E = -4.0 \text{ kcal/mol} \quad (1)$$

$$TiO_2(^1A_1) + CO_2(^1\Sigma_g^+) \rightarrow OTiCO_3(^1A') \quad DE = -24.7 \text{ kcal/mol} \quad (2)$$

The $TiO_2(\eta^1$-CO) complex absorptions were produced at the expense of the TiO(η^1-OCO) absorptions under visible light irradiation, which suggests that the $TiO_2(\eta^1$-CO) complex is formed from TiO(η^1-OCO). This isomerization reaction process proceeded under visible light excitation, indicating that the reaction requires activation energy, and that some excited states may be involved in this process. The TiO molecule has a high density of allowed transitions in the visible region for excitation of the metal monoxide in the TiO(η^1-OCO) complex.[42]

The potential energy profile along the $TiO + CO_2 \rightarrow TiO_2(\eta^1$-CO) reaction path was calculated, and the results are shown in Figure 9. The initial step of the reaction is the

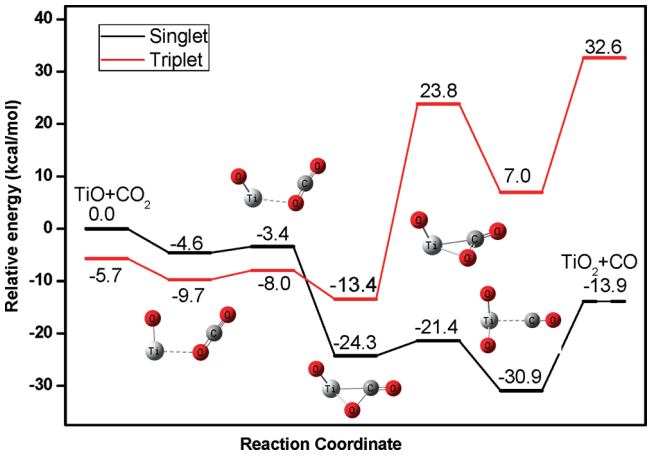

Figure 9. Potential energy profile of the $TiO + CO_2 \rightarrow TiO_2 + CO$ reaction calculated at the B3LYP/6-311+G(2df) level. Relative energies (kcal/mol) are calculated at 0 K and are corrected with zero-point vibrational energy.

formation of the TiO(η^1-OCO) complex, which was predicted to be exothermic by 4.0 kcal/mol and is barrier-free. From TiO(η^1-OCO), one O atom transfers from CO_2 to the metal center to form the $TiO_2(\eta^1$-CO) isomer. Because the TiO(η^1-OCO) complex has a triplet ground state, whereas the $TiO_2(\eta^1$-CO) isomer has a singlet ground state, there is spin crossing from triplet TiO(η^1-OCO) to singlet $TiO_2(\eta^1$-CO). The geometry of the crossing point can be roughly determined by the following procedure: (1) Perform IRC calculations on both the singlet and triplet potential energy surfaces. (2) Perform single-point-energy calculation with triplet state using the geometries optimized along the IRC of the singlet potential energy surface. (3) Perform single-point-energy calculation with the singlet state using the geometries optimized along the

Table 5. Observed Neon Matrix and Calculated (B3LYP/6-311+G(2df)) Vibrational Frequencies (cm^{-1}) for $OTiCO_3$ (B)[a]

	$OTiCO_3$		$OTi^{13}CO_3$		$^{16}OTi^{16}OC^{18}O_2$	
mode	obs	calcd	obs	calcd	obs	calcd
CO str	1825.9	1853.8(664)	1768.3	1807.1	1785.7	1817.7
Ti═O str	1012.9	1065.7(327)	1012.9	1065.6	1012.6	1065.4
CO asym str	1029.9	1037.7(266)	1000.5	1012.5	1018.2	1028.1
CO sym str	903.7	928.3(80)	900.5	925.0	877.0	897.7
CO_2 bending	819.5	830.4(158)	817.1	828.4	800.2	810.0
CO_2 bending	784.3	792.5(32)	762.2	769.4	775.5	784.1
OTiO str	458.5	456.8(61)	456.1	454.4	450.0	448.2

[a]The intensities are listed in parentheses in km/mol. Only the vibrations above 400 cm^{-1} are listed.

dx.doi.org/10.1021/jp301025n | J. Phys. Chem. A 2012, 116, 3388−3395

IRC of the triplet potential energy surface. The crossing point was then determined to have a TiO bond length between 2.08 and 2.13 Å. The isomerization reaction was predicted to be exothermic by 21.2 kcal/mol and proceeds via a OTi(η^2-O,C)O intermediate. Experimentally, the OTi(η^2-O,C)O intermediate was not observed. As can be seen from Figure 9, the formation of OTi(η^2-O,C)O from TiO(η^1-OCO) is quite exothermic, whereas its rearrangement to TiO_2(η^1-CO) exhibits a very low energy barrier (2.9 kcal/mol). Similar CO_2 reduction to CO bound on a metal center has been observed in the NbO + CO_2 reaction.[22] In general, CO_2 can be reduced to CO at electron-rich metal centers with the concomitant formation of strong metal−oxygen bond to compensate for overcoming the high enthalpy of the C═O bond of carbon dioxide.[43]

Because the TiO_2 + CO_2 reaction prefers to form $OTiCO_3$ carbonate complex, we also calculated the potential energy profile for the TiO + CO_2 → $TiCO_3$ reaction path. As can be seen in Figure 10, the formation of carbonate complex is both

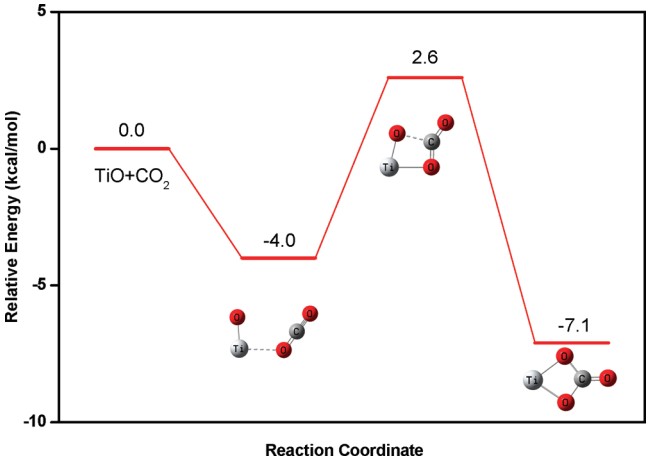

Figure 10. Potential energy profile of the TiO + CO_2 → $TiCO_3$ reaction calculated at the B3LYP/6-311+G(2df) level. Relative energies (kcal/mol) are calculated at 0 K and are corrected with zero-point vibrational energy.

thermodynamically and kinetically unfavorable with respect to the formation of TiO_2(η^1-CO).

The potential energy profile along the TiO_2 + CO_2 → $OTiCO_3$ reaction path also was calculated, and the results are shown in Figure 11. CO_2 interacts with TiO_2 to form a TiO_2(η^1-OCO) complex. Formation of this complex was predicted to be exothermic by 13.4 kcal/mol and is barrier-free. The complex has no symmetry with the CO_2 ligand end-on bonded to the titanium center via one O atom. Due to increased electrostatic interaction, the TiO_2(η^1-OCO) complex is more strongly bound than the TiO(η^1-OCO) complex. The reaction from TiO_2(η^1-OCO) to $OTiCO_3$ proceeded via a transition state lying only 1.4 kcal/mol higher in energy that the TiO_2(η^1-OCO) complex. The overall reaction was predicted to be exothermic by 24.7 kcal/mol and proceeds via one transition state lying 12.0 kcal/mol lower in energy than the ground state reactants. The exothermicity of the overall reaction and the negative energy barrier height as compared to the reactants imply that the TiO_2 + CO_2 → $OTiCO_3$ is both thermodynamically favorable and spontaneous in each kinetic steps. Owing to the small barriers, the TiO_2(η^1-OCO) complex intermediate cannot be trapped in the solid neon matrix.

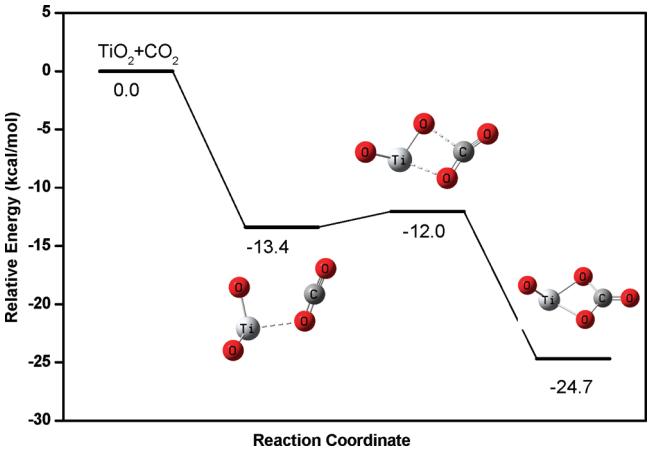

Figure 11. Potential energy profile of the TiO_2 + CO_2 → $OTiCO_3$ reaction calculated at the B3LYP/6-311+G(2df) level. Relative energies (kcal/mol) are calculated at 0 K and are corrected with zero-point vibrational energy.

CONCLUSIONS

Carbon dioxide coordination and activation by titanium monoxide and dioxide molecules were investigated by matrix isolation infrared spectroscopy as well as DFT calculations. The ground state TiO molecule reacted with carbon dioxide in solid neon to form the TiO(η^1-OCO) complex spontaneously on annealing, which was characterized to be an end-on η^1-O bonded complex. Under visible excitation, the TiO(η^1-OCO) complex rearranged to the TiO_2(η^1-CO) isomer, in which CO_2 is reduced to CO bound on a TiO_2 center. The titanium dioxide molecule was found to react with carbon dioxide in forming the $OTiCO_3$ complex spontaneously on annealing. The $OTiCO_3$ complex was characterized to be an oxo titanium carbonate complex with the CO_3 fragment bound to the Ti center in a η^2-O,O side-on fashion. Theoretical calculations predicted that both the TiO + CO_2 → TiO_2(η^1-CO) and TiO_2 + CO_2 → $OTiCO_3$ reactions are thermodynamically exothermic and kinetically facile.

ASSOCIATED CONTENT

Supporting Information

Complete ref 33. This material is available free of charge via the Internet at http://pubs.acs.org.

AUTHOR INFORMATION

Corresponding Author

*Fax: (+86) 21-6564-3532. E-mail: M.Z., mfzhou@fudan.edu.cn; Z.H.L., lizhenhua@fudan.edu.cn.

Notes

The authors declare no competing financial interest.

ACKNOWLEDGMENTS

We gratefully acknowledge finical support from National Natural Science Foundation of China (Grant No. 20933003, 21173053 and 20973041) and National Basic Research Program of China (2009CB623506 and 2010CB732306).

REFERENCES

(1) Dheandhanoo, S.; Chatterjee, B. K.; Johnson, R. *J. Chem. Phys.* **1985**, *83*, 3327−3329.

(2) Wesendrup, R.; Schwarz, H. *Angew. Chem., Int. Ed. Engl.* **1995**, *34*, 2033−2035.

(3) Sievers, M. R.; Armentrout, P. B. *J. Chem. Phys.* **1995**, *102*, 754−762.
(4) (a) Griffin, J. B.; Armentrout, P. B. *J. Chem. Phys.* **1998**, *108*, 8075−8083. (b) Zhang, X. G.; Armentrout, P. B. *J. Phys. Chem. A* **2003**, *107*, 8904−8914.
(5) (a) Sievers, M. R.; Armentrout, P. B. *Int. J. Mass Spectrom.* **1998**, *179/180*, 103−115. (b) Sievers, M. R.; Armentrout, P. B. *J. Phys. Chem. A* **1998**, *102*, 10754−10762. (c) Sievers, M. R.; Armentrout, P. B. *Inorg. Chem.* **1999**, *38*, 397−402. (d) Zhang, X. G.; Armentrout, P. B. *J. Phys. Chem. A* **2003**, *107*, 8915−8922.
(6) Koyanagi, G. K.; Bohme, D. K. *J. Phys. Chem. A* **2006**, *110*, 1232−1241.
(7) (a) Campbell, M. L. *Phys. Chem. Chem. Phys.* **1999**, *1*, 3731−3735. (b) Campbell, M. L. *Chem. Phys. Lett.* **2000**, *330*, 547−550.
(8) Larsson, R.; Mascetti, J. *React. Kinet. Catal. Lett.* **2005**, *85*, 107−113.
(9) (a) Mascetti, J.; Tranquille, M. *J. Phys. Chem.* **1988**, *92*, 2177−2184. (b) Galan, F.; Fouassier, M.; Tranquille, M.; Mascetti, J.; Papai, I. *J. Phys. Chem. A* **1997**, *101*, 2626−2633. (c) Mascetti, J.; Galan, F.; Papai, I. *Coord. Chem. Rev.* **1999**, *190−192*, 557−576.
(10) (a) Souter, P. F.; Andrews, L. *Chem. Commun.* **1997**, 777−778. (b) Souter, P. F.; Andrews, L. *J. Am. Chem. Soc.* **1997**, *119*, 7350−7360.
(11) (a) Zhou, M. F.; Andrews, L. *J. Am. Chem. Soc.* **1998**, *120*, 13230−13239. (b) Zhou, M. F.; Andrews, L. *J. Phys. Chem. A* **1999**, *103*, 2066−2075. (c) Zhou, M. F.; Liang, B. Y.; Andrews, L. *J. Phys. Chem. A* **1999**, *103*, 2013−2023.
(12) (a) Zhang, L. N.; Wang, X. F.; Chen, M. H.; Qin, Q. Z. *Chem. Phys.* **2000**, *254*, 231−238. (b) Chen, M. H.; Wang, X. F.; Zhang, L. N.; Qin, Q. Z. *J. Phys. Chem. A* **2000**, *104*, 7010−7015. (c) Wang, X. F.; Chen, M. H.; Zhang, L. N.; Qin, Q. Z. *J. Phys. Chem. A* **2000**, *104*, 758−764.
(13) (a) Liang, B. Y.; Andrews, L. *J. Phys. Chem. A* **2002**, *106*, 595−602. (b) Liang, B. Y.; Andrews, L. *J. Phys. Chem. A* **2002**, *106*, 4042−4053.
(14) Andrews, L.; Zhou, M. F.; Liang, B. Y.; Li, J.; Bursten, B. E. *J. Am. Chem. Soc.* **2000**, *122*, 11440−11449.
(15) (a) Jiang, L.; Zhang, X. B.; Han, S.; Xu, Q. *Inorg. Chem.* **2008**, *47*, 4826−4831. (b) Jiang, L.; Teng, Y. L.; Xu, Q. *J. Phys. Chem. A* **2007**, *111*, 7793−7799. (c) Jiang, L.; Xu, Q. *J. Phys. Chem. A* **2007**, *111*, 3519−3525.
(16) (a) Sodupe, M.; Branchadell, V.; Oliva, A. *J. Phys. Chem.* **1995**, *99*, 8567−8571. (b) Sodupe, M.; Branchadell, V.; Rosi, M.; Bauschlicher, C. W. Jr. *J. Phys. Chem. A* **1997**, *101*, 7854−7859.
(17) (a) Hwang, D. Y.; Mebel, A. M. *Chem. Phys. Lett.* **2002**, *357*, 51−58. (b) Hwang, D. Y.; Mebel, A. M. *J. Chem. Phys.* **2002**, *116*, 5633−5642. (c) Hwang, D. Y.; Mebel, A. M. *J. Phys. Chem. A* **2000**, *104*, 11622−11627.
(18) (a) Papai, I.; Schubert, G.; Hannachi, Y.; Mascetti, J. *J. Phys. Chem. A* **2002**, *106*, 9551−9557. (b) Papai, I.; Mascetti, J.; Fournier, R. *J. Phys. Chem. A* **1997**, *101*, 4465−4471. (c) Papai, I.; Hannachi, Y.; Gwizdala, S.; Mascetti, J. *J. Phys. Chem. A* **2002**, *106*, 4181−4186. (d) Hannachi, Y.; Mascetti, J.; Stirling, A.; Papai, I. *J. Phys. Chem. A* **2003**, *107*, 6708−6713.
(19) (a) Wang, Y. C.; Yang, X. Y.; Geng, Z. Y.; Liu, Z. Y.; Chen, X. X.; Gao, L. G. *Acta Chim. Sinica* **2006**, *64*, 2310−2316. (b) Dai, G. L.; Wang, C. F. *THEOCHEM* **2009**, *909*, 122−128.
(20) (a) Chen, X. Y.; Zhao, Y. X.; Wang, S. G. *J. Phys. Chem. A* **2006**, *110*, 3552−3558. (b) Musaev, D. G.; Irle, S.; Lin, M. C. *J. Phys. Chem. A* **2007**, *111*, 6665−6673.
(21) Hossain, E.; Rothgeb, D. W.; Jarrold, C. C. *J. Chem. Phys.* **2010**, *133*, 024305.
(22) Zhou, M. F.; Zhou, Z. J.; Zhuang, J.; Li, Z. H.; Fan, K. N.; Zhao, Y. Y.; Zheng, X. M. *J. Phys. Chem. A* **2011**, *115*, 14361−14369.
(23) (a) Indrakanti, V. P.; Kubicki, J. D.; Schobert, H. H. *Energy Environ. Sci* **2009**, *2*, 745−758. (b) Woolerton, T. W.; Sheard, S.; Reisner, E.; Pierce, E.; Ragsdale, S. W.; Armstrong, F. A. *J. Am. Chem. Soc.* **2010**, *132*, 2132−2133.
(24) (a) Burghaus, U. *Catal. Today* **2009**, *148*, 212−220. (b) He, H. Y.; Zapol, P.; Curtiss, L. A. *J. Phys. Chem. C* **2010**, *114*, 21474−21481. (c) Indrakanti, V. P.; Kubicki, J. D.; Schobert, H. H. *Energy Fuels* **2008**, *22*, 2611−2618.
(25) (a) Zhou, M. F.; Zhang, L. N.; Shao, L. M.; Wang, W. N.; Fan, K. N.; Qin, Q. Z. *J. Phys. Chem. A* **2001**, *105*, 10747−10752. (b) Zhou, M. F.; Zhang, L. N.; Qin, Q. Z. *J. Phys. Chem. A* **2001**, *105*, 6407−6413.
(26) (a) Wang, G. J.; Chen, M. H.; Zhou, M. F. *J. Phys. Chem. A* **2004**, *108*, 11273−11278. (b) Wang, G. J.; Gong, Y.; Chen, M. H.; Zhou, M. F. *J. Am. Chem. Soc.* **2006**, *128*, 5974−5980. (c) Wang, G. J.; Chen, M. H.; Zhao, Y. Y.; Zhou, M. F. *Chem. Phys.* **2006**, *322*, 354−359. (d) Wang, G. J.; Lai, S. X.; Chen, M. H.; Zhou, M. F. *J. Phys. Chem. A* **2005**, *109*, 9514−9520. (e) Huang, Y. F.; Zhao, Y. Y.; Zheng, X. M.; Zhou, M. F. *J. Phys. Chem. A* **2010**, *114*, 2476−2482.
(27) (a) Zhou, M. F.; Wang, C. X.; Li, Z. H.; Zhuang, J.; Zhao, Y. Y.; Zheng, X. M.; Fan, K. N. *Angew. Chem., Int. Ed.* **2010**, *49*, 7757−7761. (b) Wang, C. X.; Zhuang, J.; Wang, G. J.; Chen, M. H.; Zhao, Y. Y.; Zheng, X. M.; Zhou, M. F. *J. Phys. Chem. A* **2010**, *114*, 8083−8089. (c) Zhao, Y. Y.; Huang, Y. F.; Zheng, X. M.; Zhou, M. F. *J. Phys. Chem. A* **2010**, *114*, 5779−5786. (d) Zhou, M. F.; Wang, C. X.; Zhuang, J.; Zhao., Y. Y.; Zheng, X. M. *J. Phys. Chem. A* **2011**, *115*, 39−46.
(28) Wang, G. J.; Zhou, M. F. *Int. Rev. Phys. Chem.* **2008**, *27*, 1−25.
(29) (a) Becke, A. D. *J. Chem. Phys.* **1993**, *98*, 5648−5652. (b) Lee, C.; Yang, W.; Parr, R. G. *Phys. Rev. B* **1988**, *37*, 785−789.
(30) (a) McLean, A. D.; Chandler, G. S. *J. Chem. Phys.* **1980**, *72*, 5639−5648. (b) Krishnan, R.; Binkley, J. S.; Seeger, R.; Pople, J. A. *J. Chem. Phys.* **1980**, *72*, 650−654.
(31) (a) Cramer, C. J.; Truhlar, D. G. *Phys. Chem. Chem. Phys.* **2009**, *11*, 10757−10816. (b) Sousa, S. F.; Fernandes, P. A.; Ramos, M. J. *J. Phys. Chem. A* **2007**, *111*, 10439−10452.
(32) Peng, C.; Ayala, P. Y.; Schlegel, H. B.; Frisch, M. J. *J. Comput. Chem.* **1996**, *17*, 49−56.
(33) Frisch, M. J.; Trucks, G. W.; Schlegel, H. B.; Scuseria, G. E.; Robb, M. A.; Cheeseman, J. R.; Scalmani, G.; Barone, V.; Mennucci, B.; Petersson, G. A.;et al. *Gaussian 09*, Revision A.02; Gaussian, Inc.: Wallingford, CT, 2009.
(34) (a) Chertihin, G. V.; Andrews, L. *J. Phys. Chem.* **1995**, *99*, 6356−6366. (b) Gong, Y.; Zhou, M. F.; Andrews, L. *Chem. Rev.* **2009**, *109*, 6765−6808.
(35) (a) Gong, Y.; Zhou, M. F.; Tian, S. X.; Yang, J. L. *J. Phys. Chem. A* **2007**, *111*, 6127−6130. (b) Gong, Y.; Zhou, M. F. *J. Phys. Chem. A* **2008**, *112*, 9758−9762. (c) Gong, Y.; Zhang, Q. Q.; Zhou, M. F. *J. Phys. Chem. A* **2007**, *111*, 3534−3539.
(36) (a) Ramis, G.; Busca, G.; Lorenzelli, V. *Mater. Chem. Phys.* **1991**, *29*, 425−435. (b) Henderson, M. A. *Surf. Sci.* **1998**, *400*, 203−219.
(37) (a) Foster, J. P.; Weinhold, F. *J. Am. Chem. Soc.* **1980**, *102*, 7211−7218. (b) Reed, A. E.; Weinhold, F. *J. Chem. Phys.* **1985**, *83*, 1736−1740. (c) Reed, A. E.; Weinstock, R. B.; Weinhold, F. *J. Chem. Phys.* **1985**, *83*, 735−746. (d) Reed, A. E.; Curtiss, L. A.; Weinhold, F. *Chem. Rev.* **1988**, *88*, 899−926.
(38) Zhou, M. F.; Andrews, L.; Bauschlicher, C. W. Jr. *Chem. Rev.* **2001**, *101*, 1931−1961.
(39) (a) Lupinetti, A. J.; Frenking, G.; Strauss, S. H. *Angew. Chem., Int. Ed.* **1998**, *37*, 2113−2116. (b) Lupinetti, A. J.; Strauss, S. H.; Frenking, G. *Prog. Inorg. Chem.* **2001**, *49*, 1−112. (c) Goldman, A. S.; Krogh-Jespersen, K. *J. Am. Chem. Soc.* **1996**, *118*, 12159−12166.
(40) Ricks, A. M.; Reed, Z. D.; Duncan, M. A. *J. Mol. Spectrosc.* **2011**, *266*, 63−74.
(41) Krishnamurty, K. V.; Harris, G. M.; Sastri, V. S. *Chem. Rev.* **1970**, *70*, 171−197.
(42) (a) Huber, K. P.; Herzberg, G. *Constants of Diatomic Molecules*; Van Nostrand Reinhold: New York, 1979. (b) Barnes, M.; Merer, A. J.; Metha, G. F. *J. Mol. Spectrosc.* **1997**, *181*, 180−193.
(43) (a) Castro-Rodriguez, I.; Meyer, K. *J. Am. Chem. Soc.* **2005**, *127*, 11242−11243. (b) Lu, C. C.; Saouma, C. T.; Day, M. W.; Peters, J. C. *J. Am. Chem. Soc.* **2007**, *129*, 4−5. (c) Laitar, D. S.; Muller, P.; Sadighi, J. P. *J. Am. Chem. Soc.* **2005**, *127*, 17196−17197.